Analytical Methods

Accepted Manuscript

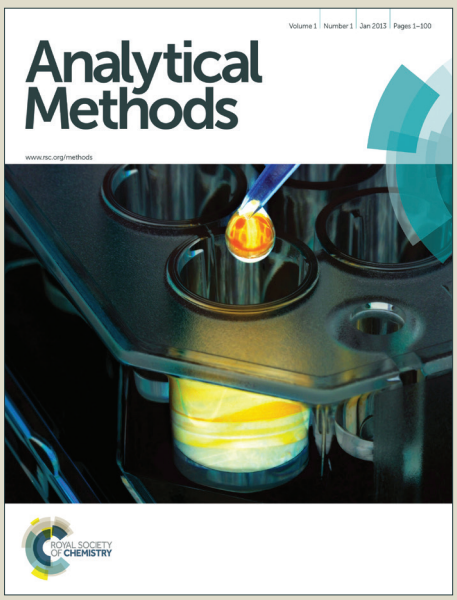

ROYAL SOCIETY OF CHEMISTRY

www.rsc.org/methods

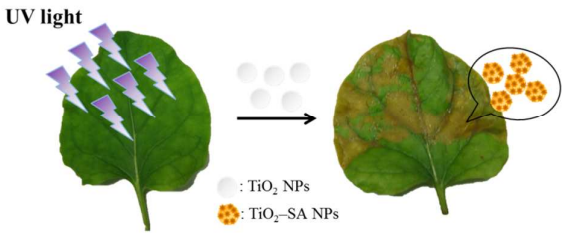

Colorimetric sensing salicylic acid in tobacco leaves *in situ* using TiO_2 NPs

Journal Name

RSCPublishing

ARTICLE

A facile colorimetric assay for determination of salicylic acid in tobacco leaves using titanium dioxide nanoparticles

Cite this: DOI: 10.1039/x0xx00000x

Received 00th January 2012,
Accepted 00th January 2012

DOI: 10.1039/x0xx00000x

www.rsc.org/

Po-Jen Tseng[a], Chiung-Yi Wang[a], Zi-Yun Huang[a], Yuan-Yu, Zhuang[a], Shih-Feng Fu[b] and Yang-Wei Lin[a,*]

A facile, colorimetric method for salicylic acid (SA) detection in tobacco leaves was developed using titanium dioxide nanoparticles (TiO_2 NPs). The sensing strategy is based on the reaction of TiO_2 NPs with SA at pH 5.5, which results in an intramolecular ligand to metal charge transfer transition between salicylate and Ti(IV) on the surface of TiO_2 NPs, and causes the TiO_2 NPs solution to turn yellow. The TiO_2 NPs probe exhibits high selectivity for SA over seven structural chemicals (4-hydroxybenzoic acid, 3-hydroxybenzoic acid, benzoic acid, acetylsalicylic acid, phenol, methyl salicylate, and jasmonic acid). Moreover, the difference in the absorbance of the TiO_2 NPs solution is proportional to the concentration of SA over the range from 0.02 to 1.0 mM ($R^2 = 0.992$). By using the TiO_2 NPs probe in 5 mM sodium acetate (pH 5.5) solutions, the limit of detection for SA was 15.4 μM at a signal-to-noise (S/N) ratio of 3. Furthermore, the practicality of the TiO_2 NPs probe was validated for the determination of SA in tobacco leaves by demonstrating its advantages, including simplicity, and selectivity.

Introduction

Salicylic acid (SA; 2-hydroxybenzoic acid) has been shown to play an important role in plant for heat production, flowering, and germination processes.[1-4] Moreover, it has been found to be a key compound for pathogen resistance and the associated signal transduction.[5-8] Its accumulation can induce immune responses such as age-related resistance and systemic acquired resistance (SAR), and gene expression associated with these responses.[9-11] It can also contribute to the hypersensitive response (HR), which is the action of programmed cell death induces signals to restrict pathogen spreading.[12-15] Therefore, it is necessary to quantify SA routinely in the field of plant immunity.[16]

To date, quantitative detection of SA in plant tissue is achieved using liquid chromatography.[17-19] The technique involves extraction of SA into organic solvents, followed by chromatographic separation and detection via spectroscopy. More recently, the concentration of SA has been further determined by mass spectroscopy (MS).[20-24] In some research, the use of an enzyme-linked immunosorbent assay method has been reported for the quantitative analysis of SA in plant extracts.[25, 26] These methods are highly accurate, quantitative and can be adapted for high throughput analysis of many samples; however, the extraction and purification of SA is laboratory intensive.[27] They are also destructive and cannot provide information on the spatial distribution of SA within plant tissues. Recently, Huang *et al.* demonstrated the SA biosensor *Acinetobacter* sp. ADPWH_*lux*.[28, 29] This strain which contains a chromosomal integration of a salicylate inducible *lux*CDABE operon provides the substrate and catalyst for SA luminescence. Measurement of SA from tobacco mosaic virus (TMV) –infected tobacco leaves using the biosensor and MS found similar results, demonstrating that this strain is adequate to determination of SA in plant *in vivo*. However, the reaction time should take 2 hr prior to image and this biosensor is laboratory intensive.

Herein, we report a facile, colorimetric detection method for SA in tobacco leaves using a nanoparticle-based sensor. In recent years, the study of metal oxide particles with well-defined nanostructures has become one of the most active research areas. Titanium dioxide nanoparticles (TiO_2 NPs) are representative materials that have received considerable attention for use in dye-sensitized photovoltaic cells and photocatalysis.[30, 31] In addition, the surface charge-transfer complexes between TiO_2 NPs and enediols have been reported.[32, 33] As mentioned in the study, upon photoexcitation, an electron is considered to be transferred from the HOMO of the enediols to the conduction band of the TiO_2 through the LUMO of the enediols. Besides the intrinsic interest of these systems for studying electron-transfer processes, these enediols also act as surface photosensitizers, enabling the TiO_2 to absorb and respond to visible light region.[34-36] SA has an enediol-type

structure; the possibility of its quantitative detection using TiO_2 NPs was therefore investigated. The effects of the buffer systems and the quantity of TiO_2 NPs on the selectivity and sensitivity for the detection of SA were evaluated. The practicality of the TiO_2 NPs sensor was then validated for the detection of SA in tobacco leaf extracts. Finally, tobacco leaves were immersed in a solution of TiO_2 NPs to determine the spatial distribution of SA levels with and without the appearance of the HR elicited by UV irradiation in an *NN* genotype tobacco. These results indicate that the TiO_2 NPs sensor is potentially useful for the non-destructive visualization of changes in the SA content in plant tissues.

Experimental sections

Materials

Titanium(IV) isopropoxide, SA, acetylsalicylic acid (AA), sodium hydroxide, sodium acetate, jasmonic acid (JA), acetic acid, and acetonitrile were obtained from Sigma (St. Louis, MO, USA), and 4-hydroxybenzoic acid (4-HBA), 3-hydroxybenzoic acid (3-HBA), benzoic acid (BA), methyl salicylate (MeS), nitric acid, ethyl acetate, cyclohexane, boric acid and sodium phosphate were obtained from Acros (Morris Plains, NJ, USA). Phenol (ph) was purchased from Tokyo Chemical Industry (Tokyo, Japan), and trichloroacetic acid and methanol were obtained from Fluka (Ronkonkoma, NY, USA).

Apparatus

UV-Vis absorption spectra of the TiO_2 NPs in the absence and presence of SA were recorded using a Synergy H1 Hybrid Multi-Mode Microplate Reader (Biotek Instruments, Winooski, VT, USA). UV-Vis diffuse reflectance spectra of the samples were measure by using an Evolution 220 UV-Vis spectrophotometer (Thermo Scientific Inc., NY, USA). A JEOL-1200EX II transmission electron microscopy system (JEOL, Tokyo, Japan) was used to measure the size and shape of the TiO_2 NPs in the absence and presence of SA. The Raman spectrum of the TiO_2 NPs in the presence of SA was recorded using a DXR Raman Microscope (Thermo Scientific Inc., NY, USA). Microflex matrix-assisted laser desorption/ionization-time of flight mass spectrometer (MS) experiment was performed in the negative ion mode (MALDI-TOF-MS, Bruker Daltonics, Bremen, Germany). The hydrodynamic diameters and zeta potentials of the TiO_2 NPs in the presence of SA were measured using a Zetasizer Nano ZS90 apparatus (Malvern, UK). A high-voltage power supply (Gamma High Voltage Research, Ormond Beach, FL, USA) was used to drive electrophoresis. The CE system was coupled to a variable wavelength UV detector (SAPPHIRE 600, ECOM, Praha, Czech Republic). Data acquisition and processing were accomplished using a PC equipped with a Peak-ABC Chromatography Data Handling System (Shanghai Qianpu Software Company Ltd., Shanghai, China).

Preparation of TiO_2 NPs

The TiO_2 NPs were prepared via a sol–gel reaction according to a previously described procedure.[36] Titanium isopropoxide (10 mL) was added to 0.1 M nitric acid (60 mL) with vigorous stirring at 80°C, and a white precipitate formed instantaneously. After that, the slurry was heated at 80°C and stirred vigorously for 8 h, leading to the formation of a sol and then a colloidal solution. The concentration of the as-prepared TiO_2 NPs was estimated to be 240 μM (2×10^{17} particles/mL) by assuming that the titanium isopropoxide reacted completely to form TiO_2 NPs.[36]

General procedure for colorimetric analysis

A stock solution of SA (10 mM) prepared in deionized (D.I.) water was diluted to 0 – 1.0 mM, and each dilution was added to a 5 mM sodium acetate buffer solution (pH 5.5) containing 24 μM TiO_2 NPs to give a final volume of 1000 μL. For selective determination of SA, seven structural analogues (4-HBA, 3-HBA, BA, AA, ph, MeS, and JA (1.0 mM each)) were each added to a 5 mM sodium acetate buffer (pH 5.5) solution containing 24 μM TiO_2 NPs to give a final volume of 1000 μL. After equilibration at ambient temperature for 5 min, the mixtures were transferred separately into 96-well microtiter plate and their UV-Vis spectra were recorded. Determinations were performed in triplicate for three preparations of the samples.

Determination of SA by capillary electrophoresis

The concentration of SA by capillary electrophoresis (CE) with UV detection was determined according to a previously described study with slight modifications.[37] Bare fused-silica capillaries (Polymicro Technologies, Phoenix, AZ, USA) with a 75-μm I.D. and 365-μm O.D. were used for the determination of SA. Before use, new capillaries were flushed with 0.5 mol l^{-1} NaOH for 3 h, rinsed extensively with water, and finally conditioned with the separation buffer solution for 30 min. The capillary length was 45 cm, and the detection window was located 10 cm from the outlet side. When not in use, the capillaries were stored in water to prevent buffer crystallization. 20 mmol l^{-1}phosphate/boric acid solution at pH 9 in the presence of 2% methanol and 2% acetonitrile was chosen as running buffer. Each sample was injected at the elevated anode end (30 cm above the cathode) into the capillary using hydrodynamic injection over 10 s. The potential applied for the separation was +16 kV. UV detection was performed at 205 nm. Between runs, the capillary was rinsed consecutively with water and the running buffer.

Extraction of SA from tobacco leaf

The procedure used for SA extraction was based on a previously described method with slight modification.[27] Tobacco leaf samples (0.5 g) was ground using a mortar and pestle. Samples were then transferred to a 1.5 mL Eppendorf tube wherein an aliquot (1 mL) of 99% methanol was added. This extraction mixture was mixed by vortex for 5 min and then

subsequently centrifuged (12,000 g) for 10 min. The supernatant was collected in a 1.5 mL Eppendorf tube, and the pellet was resuspended in 99% methanol (0.5 mL) and resubjected to sonication and centrifugation. The supernatants were combined and centrifuged again, and then the solvents were evaporated using a SpeedVac concentrator at a high drying speed. Trichloroacetic acid (10%, 500 μL) was then added to the residue, and the solution was mixed using a vortex. Partitioning with 500 μL ethyl acetate:cyclohexane (1:1, v/v) resulted in the separation of an upper organic solvent phase containing the free SA and a lower aqueous phase containing other compounds. This partitioning was carried out twice. The combined upper layers containing the free SA were evaporated to dryness using a SpeedVac concentrator at a medium drying speed. 5 mM sodium acetate solution (pH 5.5) was then added to the residue, and the solutions (leaf extracts) were mixed using a vortex.

Procedure for SA determination in tobacco leaf extracts and tobacco leave

Tobacco leaf extracts were collected using the above method. After filtration through a 0.2 μm membrane, aliquots of the leaves extracts (100 μL) were spiked with a standard solution of SA at the desired concentrations. The spiked samples were then diluted to 1000 μL using a 5 mM, pH 5.5 sodium acetate solution containing 24 μM TiO_2 NPs. After equilibration at ambient temperature for 5 min, the mixtures were transferred separately into 96-well microtiter plates and their UV-Vis spectra were recorded using a microplate reader. Determinations were performed in triplicate for three preparations of the samples.

Tobacco (*Bicotiana tabacum L.*) *cultivar Xanthi nc* (*NN* genotype) was grown in a glasshouse and used after approximately six weeks. For determination of SA (*in situ*) in the tobacco leaves, four samples were prepared: tobacco leaves in the absence of SA (a) before and (b) after immersion in a TiO_2 NPs solution for 10 min; (c) a tobacco leaves in the presence of SA after immersion in a TiO_2 NPs solution for 10 min, where the SA was introduced into the extracellular space of the leaves via infiltration through the lower epidermis using a syringe with no fitted needle; and (d) tobacco leaves in the presence of endogenous SA after immersion in a TiO_2 NPs solution for 10 min, where the endogenous SA was induced via UV irradiation at 254 nm for 20 min.

Results and discussion

Sensing strategy

It is known that surface modification of TiO_2 NPs with SA leads to the formation of a surface charge transfer complex. The SA acts as a surface photosensitizer, enabling the TiO_2 to absorb and respond to visible light (scheme 1).[34-36] As shown in the inset of Figure 1, white TiO_2 NPs turn yellow upon immersion in a colourless solution of SA. The yellow colour is a clear indication of the formation of Ti(IV)–SA complexes.[32] Figure 1 presents the UV-Vis spectra of TiO_2 NPs in the presence and absence of SA. Spectrum (a) and (b) represent the absorption of the TiO_2 NPs and SA solutions, respectively. As can be seen, modification of the TiO_2 NPs with SA (1.0 mM) leads to an extension of the absorption of the solution into the visible region (spectrum (c)). This absorption increasing in visible region is attributed to the formation of an intramolecular ligand to metal charge transfer transition between salicylate and Ti(IV) on the surface of TiO_2 NPs.[32] Diffuse reflectance spectra of TiO_2 NPs and TiO_2 NPs with SA are also shown in Fig. S1. According to the plots, the absorption edges of TiO_2 and TiO_2 with SA occur at about 311 nm and 420 nm, respectively, due to the excitation of electrons from valence gap to conductive gap. According to the plots inset Figure S1, the band-gap energies are estimated to be 3.98 eV and 2.95 eV for TiO_2 NPs and TiO_2 NPs with SA. Therefore, wavelength at 420 nm can be used for quantitative SA concentration by using TiO_2 NPs. The TEM images in Figure S2 show that the TiO_2 NPs in the presence of SA (1.0 mM) have size similar to those in the absence of SA (average 7.1 ± 0.8 nm). However, the SA was found to have an impact on the aggregation behavior of the TiO_2 NPs, suggesting that SA adsorbs onto the surfaces of the TiO_2 NPs.[35]

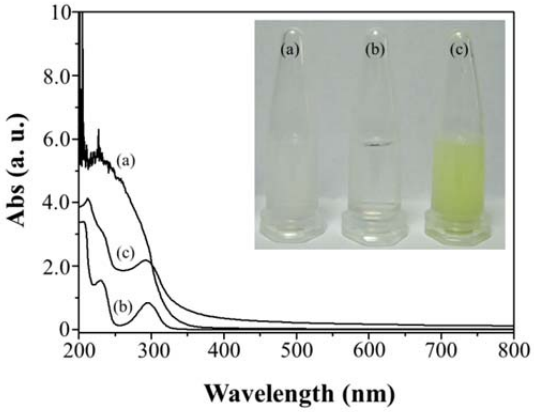

Fig. 1. UV-Vis spectra and photographic images of 5 mM, pH 5.5 sodium acetate buffer solutions of (a) 24 μM TiO_2 NPs, (b) 1.0 mM SA, and (c) 24 μM TiO_2 NPs in the presence of SA (1.0 mM).

To confirm the adsorption of SA on the surfaces of the TiO_2 NPs, Raman; MS; and dynamic light scattering analyses were performed for the TiO_2 NPs in the presence of SA after a series of centrifugation/washing steps to ensure the removal of any unbound species. Figure S3 presents the Raman spectrum obtained for the TiO_2 NPs in the presence of SA (1.0 mM). The bands at 294, 397, 510, and 627 cm^{-1} correspond to vibrations of the TiO_2 NPs; the bands in the range from 1150 to 1600 cm^{-1} correspond to the Raman resonances for adsorbed SA. The ring stretching mode is observed at 1462 cm^{-1} together with C–O stretching vibrations (coupled with ring stretching modes) at 1228, 1306, and 1592 cm^{-1}. In addition, a band appears at 1137 cm^{-1} that is associated with an in-plane CH band. Figure S4 presents the SALDI-MS spectra of SA and the TiO_2 NPs in the presence of SA (1.0 mM). The signals at m/z 136.96 and 182.94 are assigned to $[salicylate–H]^-$ and Ti(IV)–SA complex ions, respectively. Considering the mechanism shown in Scheme 1, it is possible that a Ti(IV)–SA complex exists on the surfaces of the TiO_2 NPs. A Zetasizer Nano ZS90 apparatus was employed to confirm the

adsorption of SA on the surfaces of the TiO_2 NPs that were exposed to SA (0–10 mM) at pH 5.5. It can be seen in Figure S5 that the hydrodynamic diameter of the TiO_2 NPs increased, and the zeta potential of the TiO_2 NPs became less positive with an increase in the SA concentration. These results further confirmed the possible presence of SA on the surfaces of the TiO_2 NPs. The possible reaction mechanism is presented in scheme 1. The enediol group of the SA coordinated to Ti^{4+} ions (Ti atoms) on the TiO_2 NPs surface, leading to the formation of Ti(IV)–SA coordination compounds. Upon photoexcitation, an electron is considered to be transferred from the HOMO of the SA to the conduction band of the TiO_2 through the LUMO of the SA, enabling the TiO_2 to absorb and respond to visible light region. Thus, we can determine the concentrations of SA by monitoring the increase in visible absorbance of theTiO_2 NPs.

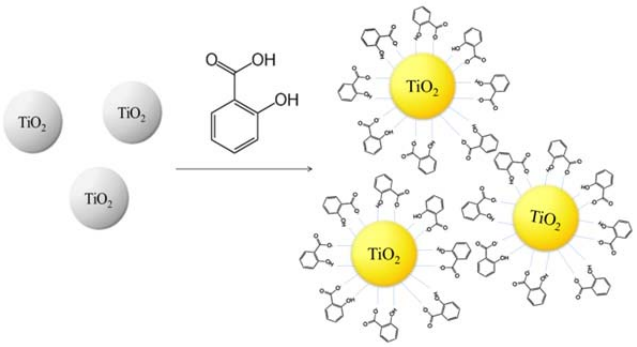

Scheme 1 Illustration of the colorimetric sensing of SA using TiO_2 NPs

Assay optimization

Additional assay parameters were then evaluated to further optimize the experimental protocol. Different concentrations of TiO_2 NPs ranging from 12 to 120 μM were tested, and it was found that the intensity of the yellow colour of the TiO_2 NPs solution in the presence of SA increased with an increase in the TiO_2 NPs concentration (inset of Figure S6). The effect of the concentration of TiO_2 NPs on the values of $(A-A_0)/A_0$, where A and A_0 represent that absorbance at 420 nm of TiO_2 NPs in the presence and the absence of SA (1.0 mM), respectively, is shown in Figure S6. The value of $(A-A_0)/A_0$ for the TiO_2 NPs decreased with an increase in the concentration of TiO_2 NPs, probably due to the inner filter effects of the TiO_2 NPs at high concentration levels. Therefore, a concentration of 24 μM was chosen as the optimal TiO_2 NPs concentration in the present study.

To test the effect of the buffer system, different buffer systems were evaluated, including sodium acetate, sodium phosphate, and tris(hydroxymethyl)aminomethane–hydrochloric acid (Tris-HCl). As can be seen in Figure S7A, the maximum difference in the absorbance for SA detection was obtained when a sodium acetate buffer was used. As we known, phosphate ions, which are adsorbed spontaneously on TiO_2 NPs, were used to modify the surface charges of metal oxides.[38] As a result, the minimum difference in the absorbance for SA detection was achieved. Therefore, the sodium acetate buffer system was selected for further study. The influence of pH was then investigated over the range from 4.5 to 8.5. For SA detection, the difference in the absorbance of the TiO_2 NPs solution increased as the pH value of the sodium acetate buffer increased up to 5.5, above which it then decreased slightly (Figure S7B), probably due to the instability of the TiO_2 NPs at higher pH. Therefore, a sodium acetate buffer at pH 5.5 was used for all further experiments. The influence of the sodium acetate buffer concentration in the range from 5 to 100 mM on the system was also tested (Figure S7C). The difference in the absorbance of the TiO_2 NPs solution decreased with an increase in the concentration of the sodium acetate buffer solution, probably due to the aggregation of the TiO_2 NPs at higher buffer concentration. Therefore, a sodium acetate concentration of 5 mM was selected as the optimal value in the follow study.

Validation of the assay

To investigate the selectivity of the TiO_2 NPs for SA (1.0 mM), seven structural analogs (4-HBA, 3-HBA, BA, AA, ph, MeS, and JA) (1.0 mM each) were added to the TiO_2 NPs (one additional substance at a time). At pH 5.5, SA induced significant increases in the absorption at 420 nm (i.e., formation of Ti(IV)–SA complexes) (Figure 2A). However, another one chemical led to a change in the absorption of the TiO_2 NPs solution: a colour change in the solution was observed for AA as a result of its hydrolysis. However, the use of 0.5% potassium fluoride as the inhibitor of AA hydrolysis was found to be effective.[39] Next, to further test the practicality of using the TiO_2 NPs as an SA sensor, analyses were conducted of mixtures containing SA (1.0 mM) and all of the seven structural analogues (4-HBA, 3-HBA, BA, AA, ph, MeS, and JA) (1.0 mM each). The results indicated that none of the structural chemicals caused any interference, and the difference in the values of the absorbance at 420 nm induced by SA in the absence and presence of the other substances was always less than 0.08 a.u. (Figure 2B).

Under optimal conditions, the sensitivity of TiO_2 NPs toward SA was then investigated. The absorbance of the Ti(IV)–SA complexes increased with an increase in the concentration of SA, and a linear relationship was obtained for the plot of the absorbance difference as a function of the concentration of SA over the range from 0.02 to 1.0 mM (R^2 = 0.992) (Figure 3). Moreover, the limit of detection of the TiO_2 NPs for SA (S/N = 3) was determined to be 15.4 μM. The UV-Vis spectra of various concentrations of SA in the absence of TiO_2 NPs were also shown in the Figure S8. There are no obvious absorbance differences in the visible region. In comparison to other optical methods, the new assay for SA is relatively rapid (5 min), and simple (no need to prepare and purify biosensor bacteria).[16, 25, 26, 28, 29]

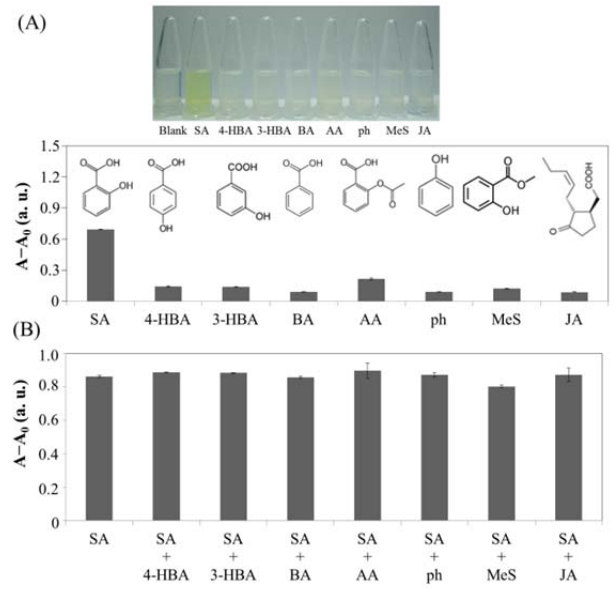

Fig. 2. (A) Selectivity of 24 μM TiO_2 NPs toward SA (n = 3). The concentration of SA was 1.0 mM, and the concentration of each of the other interferences was 1.0 mM. Inset: Photographic images of TiO_2 NPs solutions in the presence of SA and other possible interfering compounds. (B) Tolerance of 24 μM TiO_2 NPs toward SA in the presence of other possible interfering compounds (n = 3). The concentration of SA was 1.0 mM, and the concentration of each of the other substances was 1.0 mM.

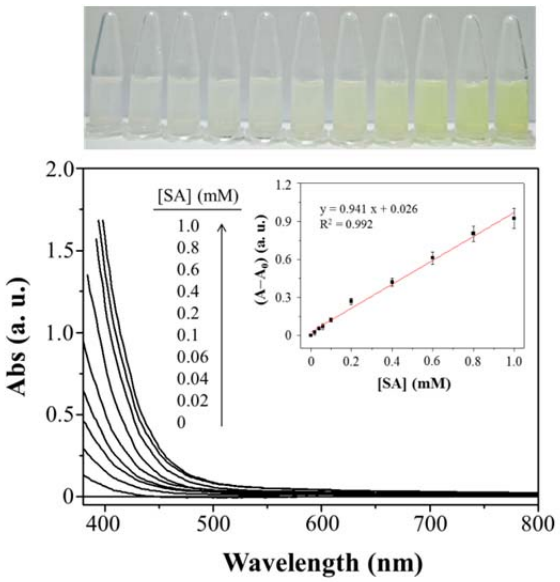

Fig.3. UV-Vis spectra and linear responses (inset) of the absorbance difference plotted with respect to the concentration of SA with TiO_2 NPs (n = 3). Photographs of 24 μM TiO_2 NPs with respect to the concentration of SA (0.02 to 1.0 mM).

Determination SA in tobacco leaf extracts and tobacco leaves *in situ*

With the expectation that the TiO_2 NPs-based sensor would have great potential for use in the analysis of SA in plant samples, a standard addition method was applied to determine the concentration of SA in a tobacco leaf extract matrix. Notably, a linear correlation was found to exist between the absorbance difference and the concentration of SA spiked in the leaf extract matrix over the range from 0.04 to 0.90 mM (R^2 = 0.997) (Figure S9). The spike recoveries for these measurements were 102.2%–104.6%. To confirm that measurements of SA obtained using TiO_2 NPs are as accurate as conventional methods, the spiked SA concentration (0.5 mM) in leaf extracts was measured using CE with UV detection. The two methods gave almost identical results: 0.52 ± 0.055 mM and 0.55 ± 0.014 mM for TiO_2 NPs probe and CE/UV methods, respectively (n = 3). Using a F-test (the F value was 19 at a 95% confidence level), the F values calculated at the 95% confidence level was 15.4, revealing that no significant differences existed between the precision of the new assay and the CE/UV method. Then, using a t-test (the t-test value was 2.776 at a 95% confidence level), the t values calculated at the 95% confidence level is 0.09. These results showed that the data obtained from the two methods were not significantly different. Our results further suggest that TiO_2 NPs probe has potential to be a quantitative *in situ* assay of SA in tobacco leaves.

Before attempting to use TiO_2 NPs to detect the endogenous SA in leaves, it was necessary to determine whether or not the TiO_2 NPs would remain capable of reporting the presence of SA following infiltration into plant leaves. Thus, SA was introduced into the extracellular space of leaves via infiltration through the lower epidermis using a syringe with no fitted needle. The leaves infiltrated with SA were then immersed in a buffer solution containing 24 μM TiO_2 NPs, and a colour change was readily detectable (photographic image c in Figure 4). On the other hand, only a slight colour change (photographic image b in Figure 4) was observed when leaves without infiltrated SA were immersed into the TiO_2 NPs solution. Next the *in situ* detection of the endogenous SA in tobacco leaves after UV irradiation (254 nm) for 20 min was demonstrated using this approach; the tobacco leaves turned yellow upon immersion in a TiO_2 NPs solution (photographic image d in Figure 4). Notably, the yellow to green ratio in the presence of SA was higher than that in the absence of SA ($P < 0.05$) (Figure 4B). This was also carried out on the same extract using the CE with UV detection. The amounts of SA found by the TiO_2 NPs and CE/UV methods were 4.14 μg mL^{-1} (SA/leaf extract) and 4.97 μg mL^{-1}, respectively. The two methods gave almost similar results. Therefore, it was concluded that TiO_2 NPs probe has potential to be used as a nanosensor for the non-destructive, *in situ* qualitative assessment and visualization of changes in SA accumulation in plant tissues. This novel probe possesses three attractive features when compared with other reported methods (Table 1): (1) expensive enzymes/substrates (ELISA), sophisticated instruments (Chromatography-MS) and complex molecular engineering (*Acinetobacter* sp. ADPWH_*lux*) are not required; (2) fast—reaction time, an intramolecular ligand to metal charge transfer transition between salicylate and TiO_2 NPs, is rapid (5 min); (3) non-destructive detection—the analysis of tobacco leaves *in situ* is possible without performing tedious sample pre-treatment.[16, 20-26, 28, 29]

Journal Name RSCPublishing

ARTICLE

Table 1 Various sensing systems for the determination of SA.

Method	Sensing system (probe)	Analytical ranges	LOD	Reaction time	*In situ* detection	Ref.
Luminescence	*Acinetobacter* sp. ADPWH_*lux*	-[a]	2.0 μM	1 hr at 37 °C	Already done	16
	Acinetobacter sp. ADPWH_*lux*	0.1–400 μM	0.1 μM	2 hr at 37 °C	Already done	28, 29
Chromatography/MS	Solid phase extraction/LC-MS/MS	3.6–362 nM	1.5 nM	15 min	Impossible	20
	HLPC-MS/MS	-[a]	7.25 pM	30 min	Impossible	21, 22
	HPLC-MS/MS	0.36–7.25 μM	3.3 nM	10 min	Impossible	23
	GC-MS/MS	72.5–109 μM	72.5 μM	10 min	Impossible	24
ELISA (absorbance)	Mouse monoclonal antibody	0.4–400 μM	0.4 μM	1.5 hr at 37 °C	Impossible	25, 26
Colorimetric	TiO_2 NPs	20–1000 μM	15.4 μM	5 min at 25 °C	Possible	This study

[a] not provided.

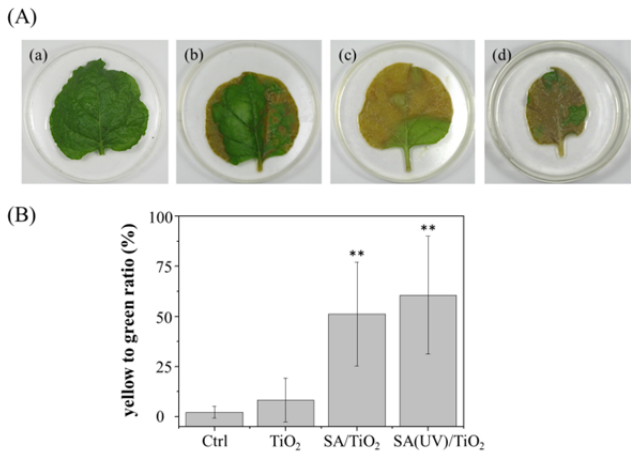

Fig. 4. (A) Photographic images and (B) statistical results (yellow to green ratio%) for tobacco leaves in the absence of SA (a) before and (b) after immersion in a 24 μM TiO_2 NPs solution; (c) tobacco leaves in the presence of SA after immersion in a 24 μM TiO_2 NPs solution (SA was introduced into the extracellular space of the leaves by infiltration through the lower epidermis using a syringe with no fitted needle); and (d) tobacco leaves in the presence of endogenous SA after immersion in a 24 μM TiO_2 NPs solution. The endogenous SA was induced via UV irradiation at 254 nm for 20 min (n = 3).

Conclusions

A facile, colorimetric method for the detection of SA in tobacco leaves using a sensor based on TiO_2 nanoparticles was described. Under optimum conditions, the TiO_2 NPs probe exhibits high selectivity for SA. Notably, the absorbance difference of the TiO_2 NPs solution is proportional to the concentration of SA over the range from 0.02 to 1.0 mM (R^2 = 0.992) with a limit of detection of 15.4 μM at a signal-to-noise (S/N) ratio of 3. The practicality of the TiO_2 NPs sensor was validated through the detection of SA in tobacco leaf extracts. Moreover, when tobacco leaves were immersed in a solution of TiO_2 NPs, the changes in the SA accumulation with and without UV light irradiation in an *NN* genotype tobacco was determined. Therefore, this new TiO_2 NPs nanosensor has potential application as a method for the non-destructive visualization of the changes in SA accumulation in plant tissues.

Acknowledgements

This study was supported by the National Science Council of Taiwan under contracts NSC 101-2113-M-018-001-MY2 and a research grant from the National Changhua University of Education for new scholars. The authors would like to thank Enago (www.enago.tw) for the English language review.

Notes and references

[a] *Department of Chemistry, National Changhua University of Education,1, Jin-De Road, Changhua City, Taiwan; Tel: 011-886-4-7232105-3522*
E-mail: linywjerry@cc.ncue.edu.tw
[b] *Department of Biology, National Changhua University of Education,1, Jin-De Road, Changhua City, Taiwan*

† Electronic Supplementary Information (ESI) available: [Figure S1. Diffuse reflectance spectra of (a) TiO_2 NPs and (b) TiO_2 NPs with SA (1.0 mM). Figure S2. TEM images of (a) 24 μM TiO_2 NPs and (b) 24 μM TiO_2 NPs in the presence of SA (1.0 mM). Figure S3. Raman spectrum of 240 μM TiO_2 NPs in the presence of SA (1.0 mM). Figure S4. SALDI-MS spectra of (a) 1.0 mM SA and (b) 24 μM TiO_2 NPs in the presence of SA (1.0 mM). Figure S5. Zeta potential and hydrodynamic diameter of 24 μM TiO_2 NPs in the presence of different concentrations of SA (0–10 mM). Figure S6. Effect of TiO_2 NPs concentration (12–120 μM) on the values for $(A-A_0)/A_0$, where A and A_0 represent that absorbance at 420 nm of TiO_2 NPs in the presence and the absence of SA (1.0 mM), respectively (n = 3). Figure S7. Effect of (A) the buffer system, (B) pH, and (C) concentration of sodium acetate buffer solution on the absorbance difference $(A-A_0)$, where A and A_0 represent the absorbance at 420 nm of TiO_2 NPs in the presence and absence of SA (1.0 mM), respectively (n = 3). Figure S8. UV-Vis spectra of various concentrations of SA (0.04 to 1.0 mM) in the absence of TiO_2 NPs. Figure S9.

Analysis of tobacco leaf extracts (aliquots spiked with SA (0.04–0.9 mM)) using 24 μM TiO_2 NPs (n = 3).]. See DOI: 10.1039/b000000x/

1. I. Raskin, I. M. Turner and W. R. Melander, *Proc. Natl. Acad. Sci. U. S. A.*, 1989, **86**, 2214-2218.
2. C. Martínez, E. Pons, G. Prats and J. León, *The Plant J.*, 2004, **37**, 209-217.
3. G. K. Sahu, in *Molecular Stress Physiology of Plants*, Springer, 2013, pp. 217-239.
4. M. Yusuf, S. Hayat, M. N. Alyemeni, Q. Fariduddin and A. Ahmad, in *SALICYLIC ACID*, Springer, 2013, pp. 15-30.
5. I. Raskin, *Annu. Rev. Plant Biol.*, 1992, **43**, 439-463.
6. D. F. Klessig and J. Malamy, in *Signals and Signal Transduction Pathways in Plants*, Springer, 1994, pp. 203-222.
7. A. M. Murphy, S. Chivasa, D. P. Singh and J. P. Carr, *Trends Plant Sci.*, 1999, **4**, 155-160.
8. T. Kawano, T. Hiramatsu and F. Bouteau, in *SALICYLIC ACID*, Springer, 2013, pp. 249-275.
9. Y. Shibata, K. Kawakita and D. Takemoto, *Mol. Plant Microbe In.*, 2010, **23**, 1130-1142.
10. M. Frias, N. Brito and C. Gonzalez, *Mol. Plant Pathol.*, 2013, **14**, 191-196.
11. S. Sharma and B. Sohal, *Appl. Bio. Res.*, 2013, **15**, 78-82.
12. Y. P. Xu, H. Y. Chen, X. Zhou and X. Z. Cai, *J. Integr. Agr.*, 2012, **11**, 1665-1674.
13. J. Jovel, M. Walker and H. Sanfacon, *Mol. Plant Microbe In.*, 2011, **24**, 706-718.
14. F. R. Rossi, A. Garriz, M. Marina, F. M. Romero, M. E. Gonzalez, I. G. Collado and F. L. Pieckenstain, *Mol. Plant Microbe In.*, 2011, **24**, 888-896.
15. W. R. de Souza, R. Vessecchi, D. J. Dorta, S. A. Uyemura, C. Curti and C. G. Vargas-Rechia, *J. Bioenerg. Biomembr.*, 2011, **43**, 237-246.
16. C. T. DeFraia, E. A. Schmelz and Z. Mou, *Plant Methods*, 2008, **4**, 28.
17. Y. L. Wu and B. Hu, *J Chromatogr A*, 2009, **1216**, 7657-7663.
18. M. Aboul-Soud, K. Cook and G. Loake, *Chromatographia*, 2004, **59**, 129-133.
19. P. M. Richardson, *Brittonia*, 1990, **42**, 115-115.
20. Y. H. Li, F. Wei, X. Y. Dong, J. H. Peng, S. Y. Liu and H. Chen, *Phytochem. Anal.*, 2011, **22**, 442-449.
21. X. Pan, R. Welti and X. Wang, *Nat. Protoc.*, 2010, **5**, 986-992.
22. X. Q. Pan and X. M. Wang, *J. Chromatogr. B*, 2009, **877**, 2806-2813.
23. G. Segarra, O. Jáuregui, E. Casanova and I. Trillas, *Phytochemistry*, 2006, **67**, 395-401.
24. E. A. Schmelz, J. Engelberth, H. T. Alborn, P. O'Donnell, M. Sammons, H. Toshima and J. H. Tumlinson, *Proc. Natl. Acad. Sci. U. S. A.*, 2003, **100**, 10552-10557.
25. S. Wang, L. Xu, G. Li, P. Chen, K. Xia and X. Zhou, *Plant Sci.*, 2002, **162**, 529-535.
26. S. Wang, G. Li, K. Xia, L. Xu, P. Chen and X. Zhou, *Acta Bot. Sin.*, 2001, **43**, 1207-1210.
27. M. C. Verberne, N. Brouwer, F. Delbianco, H. J. Linthorst, J. F. Bol and R. Verpoorte, *Phytochem. Anal.*, 2002, **13**, 45-50.
28. W. E. Huang, L. Huang, G. M. Preston, M. Naylor, J. P. Carr, Y. Li, A. C. Singer, A. S. Whiteley and H. Wang, *The Plant J.*, 2006, **46**, 1073-1083.
29. W. E. Huang, H. Wang, H. Zheng, L. Huang, A. C. Singer, I. Thompson and A. S. Whiteley, *Environ. Microbiol.*, 2005, **7**, 1339-1348.
30. P. E. Heil, H. Kang, H. Choi and K. Kim, *Appl. Phys. a-Mater.*, 2013, **112**, 371-380.
31. J. Evans, *Chem. Ind.-London*, 2012, **76**, 11-11.
32. T. Lana-Villarreal, A. Rodes, J. M. Perez and R. Gomez, *J. Am. Chem. Soc.*, 2005, **127**, 12601-12611.
33. A. E. Regazzoni, P. Mandelbaum, M. Matsuyoshi, S. Schiller, S. A. Bilmes and M. A. Blesa, *Langmuir*, 1998, **14**, 868-874.
34. W.-W. Zhao, Z.-Y. Ma, J.-J. Xu and H.-Y. Chen, *Anal. Chem.*, 2013, **85**, 8503-8506.
35. A. S. Almusallam, Y. M. Abdulraheem, M. Shahat and P. Korah, *J. Disper. Sci. Technol.*, 2012, **33**, 728-738.
36. K. H. Lee, C. K. Chiang, Z. H. Lin and H. T. Chang, *Rapid Commun. Mass Sp.*, 2007, **21**, 2023-2030.
37. F. Xie, A. Yu, Y. Cheng, R. Qi, Q. Li, H. Liu and S. Zhang, *Chromatographia*, 2010, **72**, 1207-1212.
38. H. P. Wu, T. L. Cheng and W. L. Tseng, *Langmuir*, 2007, **23**, 7880-7885.
39. Y. Goto, K. Makino, Y. Kataoka, H. Shuto and R. Oishi, *J. Chromatogr. B*, 1998, **706**, 329-335.